# Rapid Proton−coupled Electron−transfer of Hydroquinone through Phenylenevinylene Bridges

**ARTICLE** *in* LANGMUIR · FEBRUARY 2007

Impact Factor: 4.46 · DOI: 10.1021/la061555w · Source: PubMed

# Rapid Proton-coupled Electron-transfer of Hydroquinone through Phenylenevinylene Bridges

Scott A. Trammell,*,† Dwight S. Seferos,‡ Martin Moore,† Daniel A. Lowy,‖ Guillermo C. Bazan,‡ James G. Kushmerick,†,§ and Nikolai Lebedev†

*Center for Bio-Molecular Science and Engineering, Naval Research Laboratory, Washington, District of Columbia 20375, Nova Research, Inc., Alexandria, Virginia, and Departments of Chemistry and Biochemistry and Materials, Institute for Polymers and Organic Solids, University of California, Santa Barbara, California 93106*

*Received May 31, 2006. In Final Form: October 3, 2006*

We describe the synthesis of two oligo(phenylene vinylene)s (OPVs) with a hydroquinone moiety and a thiol anchor group: 4-(2′,5′-dihydroxystyryl)benzyl thioacetate and 4-[4′-(2″,5″-dihydroxystyryl)styryl]benzyl thioacetate. Monolayers on gold of these molecules were examined by electrochemical techniques to determine the electron transfer kinetics of the hydroquinone functionality ($H_2Q$) through these delocalized tethers ("molecular wires") as a function of pH. Between pH 4 and 9, rate constants were ca. 100-fold faster than for the same $H_2Q$ functionality confined to the surface via alkane tethers. Also, in this same pH range rate constants were independent of the length of the OPV bridge. These new electroactive molecules in which the hydroquinone functionality is wired to the gold surface by means of OPV tethers should be useful platforms for constructing bioelectronic devices such as biosensors, biofuel cells, and biophotovoltaic cells with a fast response time.

## Introduction

Self-assembled monolayers (SAMs) provide structurally well-defined surfaces at controlled distances; therefore, they have been employed as modified electrodes in various studies.[1−9] SAMs have been commonly utilized for attaching proteins to an electrode surface, when constructing bioelectronic devices with redox-active biomolecules.[10−15] Direct electron transfer (ET) between proteins and electrodes is hindered whenever the electroactive cofactors are buried deep within the protein, and, hence, are in poor electronic contact with the electrode. The chemical properties of the medium, which connects the electrode to the redox site, is important since electrons must be shuttled along some conductive pathway (or they tunnel through the ET barrier) to the electrode surface. For alkanethiol tethers, the ET rate decays exponentially with distance, $k = k_0 \exp(-\beta r)$, where $k$ is the first-order ET rate constant measured at a certain distance $r$ (in angstroms), while $k_0$ is the ET rate constant at zero distance,[16] and the electron tunneling decay constant, $\beta$, is in the range of $\sim 0.8-1$ Å$^{-1}$.[16]

With the aim of increasing ET rate to the electrode, molecules containing delocalized bridges ("molecular wires") such as oligo(phenylene ethynylene) (OPE) or oligo(phenylene vinylene) (OPV) have been synthesized. Such molecules are expected to show enhanced electron tunneling, as ferrocene-terminated OPEs have $\beta$ values ranging from 0.4 to 0.6,[17,18] while ferrocene-terminated OPVs show distance-independent ET rates up to 28 Å.[19,20] Among expected advantages of these molecules is the usefulness of delocalized systems for interfacing proteins with gold electrodes; previous applications include OPE for an amine oxidase[21] and OPV for blue copper proteins.[22,23] Thiol-terminated molecules containing a quinone/hydroquinone ($Q/H_2Q$) redox couple, which is important for biological activity,[24] can serve, however, as a much more general structure for connecting photoactive proteins to electrodes in device applications.[14,25−28]

* Corresponding author: e-mail scott.trammell@nrl.navy.mil.
† Naval Research Laboratory.
‡ University of California.
§ Present address: National Institute of Standards and Technology, Gaithersburg, MD 20899.
‖ Nova Research, Inc.

(1) Finklea, H. O. Electrochemistry of Organized Monolayers of Thiols and Related Molecules on Electrodes. In *Electroanalytical Chemistry;* Bard, A. J., Rubinstein, I., Eds.; Marcel Dekker: New York, 1996; Vol. 19, pp 109−335.
(2) Smalley, J. F.; Feldberg, S. W.; Chidsey, C. E. D.; Linford, M. R.; Newton, M. D.; Liu, Y. P. *J. Phys. Chem. B* **1995**, *99*, 13141−13149.
(3) Ravenscroft, M. S.; Finklea, H. O. *J. Phys. Chem. B.* **1994**, *98*, 3843−3850.
(4) Zhang, L. T.; Lu, T. B.; Gokel, G. W.; Kaifer, A. E. *Langmuir* **1993**, *9*, 786−791.
(5) Becka, A. M.; Miller, C. J. *J. Phys. Chem. B* **1992**, *96*, 2657−2668.
(6) Chidsey, C. E. D. *Science* **1991**, *251*, 919−922.
(7) Chidsey, C. E. D.; Bertozzi, C. R.; Putvinski, T. M.; Mujsce, A. M. *J. Am. Chem. Soc.* **1990**, *112*, 4301−4306.
(8) Hong, H. G.; Park, W. *Langmuir* **2001**, *17*, 2485−2492.
(9) Hong, H. G.; Park, W. *Bull. Korean Chem. Soc.* **2005**, *26*, 1885−1888.
(10) Fedurco, M. *Coord. Chem. Rev.* **2000**, *209*, 263−331.
(11) El Kasmi, A.; Wallace, J. M.; Bowden, E. F.; Binet, S. M.; Linderman, R. J. *J. Am. Chem. Soc.* **1998**, *120*, 225−226.
(12) Katz, E.; HelegShabtai, V.; Willner, B.; Willner, I.; Buckmann, A. F. *Bioelectrochem. Bioenerg.* **1997**, *42*, 95−104.
(13) Willner, I.; Liondagan, M.; Marxtibbon, S.; Katz, E. *J. Am. Chem. Soc.* **1995**, *117*, 6581−6592.
(14) Trammell, S. A.; Wang, L. Y.; Zullo, J. M.; Shashidhar, R.; Lebedev, N. *Biosens. Bioelectron.* **2004**, *19*, 1649−1655.
(15) Jhaveri, S. D.; Trammell, S. A.; Lowy, D. A.; Tender, L. M. *J. Am. Chem. Soc.* **2004**, *126*, 6540−6541.
(16) Kaifer, A. E.; Gómez-Kaifer, M. *Supramolecular electrochemistry;* Wiley−VCH: New York, 1999; p 223.
(17) Sachs, S. B.; Dudek, S. P.; Hsung, R. P.; Sita, L. R.; Smalley, J. F.; Newton, M. D.; Feldberg, S. W.; Chidsey, C. E. D. *J. Am. Chem. Soc.* **1997**, *119*, 10563−10564.
(18) Creager, S.; Yu, C. J.; Bamdad, C.; O'Connor, S.; MacLean, T.; Lam, E.; Chong, Y.; Olsen, G. T.; Luo, J.; Gozin, M.; Kayyem, J. F. *J. Am. Chem. Soc.* **1999**, *121*, 1059−1064.
(19) Dudek, S. P.; Sikes, H. D.; Chidsey, C. E. D. *J. Am. Chem. Soc.* **2001**, *123*, 8033−8038.
(20) Sikes, H. D.; Smalley, J. F.; Dudek, S. P.; Cook, A. R.; Newton, M. D.; Chidsey, C. E. D.; Feldberg, S. W. *Science* **2001**, *291*, 1519−1523.
(21) Hess, C. R.; Juda, G. A.; Dooley, D. M.; Amii, R. N.; Hill, M. G.; Winkler, J. R.; Gray, H. B. *J. Am. Chem. Soc.* **2003**, *125*, 7156−7157.
(22) Barlow, N. L.; Webster, G.; Flemming, B.; Guo, L. B.; Burn, P. L.; Armstrong, F. A. *J. Inorg. Biochem.* **2003**, *96*, 98−98.
(23) Armstrong, F. A.; Barlow, N. L.; Burn, P. L.; Hoke, K. R.; Jeuken, L. J. C.; Shenton, C.; Webster, G. R. *Chem. Commun.* **2004**, 316−317.
(24) Chambers, J. Q. Electrochemistry of quinones. In *The Chemistry of the Quinonoid Compounds*; Patai, S., Ed.; Wiley: New York, 1974; pp 737−791.
(25) Matsumoto, K.; Nomura, K.; Tohnai, Y.; Fujioka, S.; Wada, M.; Erabi, T. *Bull. Chem. Soc. Jpn.* **1999**, *72*, 2169−2175.
(26) Katz, E. Y.; Shkuropatov, A. Y.; Vagabova, O. I.; Shuvalov, V. A. *Biochim. Biophys. Acta* **1989**, *976*, 121−128.

10.1021/la061555w CCC: $37.00 
Published on Web 12/08/2006

**Chart 1. Structures of Compounds Used in This Study**[a]

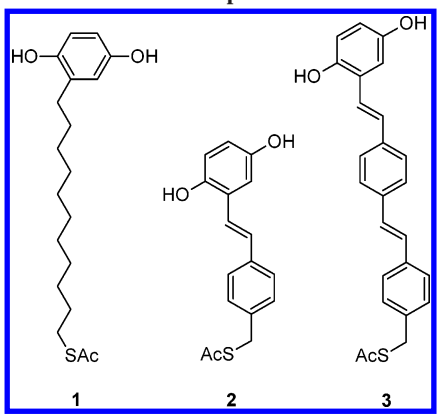


[a] See details in text.

Electrochemical properties of $Q/H_2Q$ redox couples have been studied in solution, where they display a Nernstian pH dependence, corresponding to a two-electron, two-proton couple of 59 mV/pH unit, in the range of pH 1−9, while at pH > 9.85 it displays a dependence of 28 mV/pH unit, characteristic of two-electron, one-proton couples.[29−31] Work was reported on surface-confined hydroquinones; however, these studies were limited to structures attached to an electrode via an alkane bridge[8] or a structure that contained a thiol group directly on the $H_2Q$ moiety.[32] At acidic pH, these systems display a large $\beta$ value of ∼1 per $CH_2$ unit (or 0.81 $Å^{-1}$),[8] where the rate of ET was found to rapidly decay as the $H_2Q$ is separated from the electrode surface by an increasingly long alkane chain.

In this paper we have synthesized hydroquinone−OPV−thiol molecules (Chart 1) and investigated their proton-coupled ET kinetics when they are tethered to the gold electrode surface. This study provides a foundation for understanding the role of the proton-coupled step in the ET kinetics of surface-confined hydroquinones, which is important for designing bioelectronic systems, including electrochemical biosensors, biofuel cells, and biophotovoltaic devices that are based on or contain the $Q/H_2Q$ redox couple. As compared to systems with $H_2Q$-alkane molecules, a delocalized molecular tether (including OPVs presented here) should provide more efficient coupling between the electronic features of biomolecules and the underlying electrode surface.

## Experimental Section

**Materials.** 2,5-Dimethoxybenyl chloride was obtained from Matrix Scientific. Potassium thioacetate, *n*-butyllithium, and boron tribromide were purchased from Aldrich Chemical Co. Dimethylformamide (DMF), toluene, and tetrahydrofuran (THF) used in synthetic manipulations were purified by a custom solvent purification system. Dichloromethane (DCM) was dried with calcium hydride. All other materials were reagent-grade and were used without further purification. 1,4-Dihydroxy-2-(11-thioacetate)undecylbenzene (**1**) was synthesized according to a previously reported protocol.[33]

**Synthetic Procedures: 2,5-Dimethoxybenzyltriphenylphosphonium chloride (4).**[34] In a 125 mL round-bottom flask equipped with a Teflon-coated magnetic stir bar and water-jacketed condenser, 2,5-dimethoxybenzyl chloride (2.80 g, 0.015 mol), triphenylphosphine (4.34 g, 0.016 mol), and anhydrous toluene (75 mL) were stirred vigorously at reflux for 5 h under an argon atmosphere. After cooling, filtration afforded 5.17 g (77%) of the title compound as a white crystalline solid. $^1$H NMR ($CDCl_3$) 7.61−7.79 (m, 15H), 7.08 (t, $^4J$ = 2.79 Hz, 1H), 6.75 (dt, $^3J$ = 8.93 Hz, 1H), 6.52 (d, 1H), 5.34 (d, $^{HP}J$ = 14.24 Hz, 2H), 3.59 (s, 3H), 3.16 (s, 3H).

**4-(2′,5′-Dimethoxystyryl)benzyl chloride (5) and 4-(2′,5′-Dimethoxystyryl)benzyl Bromide.** In a 125 mL round-bottom flask equipped with a Teflon-coated magnetic stir bar, sodium hydride was added to 2,5-dimethoxybenzyltriphenylphosphonium chloride (448 mg, 1.00 mmol) in THF (20 mL) at 0 °C under an argon atmosphere with vigorous stirring. After 20 min, 4-bromomethylbenzaldehyde (205 mg, 1.03 mmol) was added. After 10 min, the reaction was allowed to warm to room temperature and stirred for an additional 3.5 h. The reaction was quenched with water (10 mL), diluted with DCM (100 mL), washed with brine (3 × 50 mL), then dried, and concentrated. Chromatography on silica gel eluting with DCM in hexanes (1:1) afforded 238 mg (71%) of the title compound as a mixture of *E* and *Z* isomers (∼2:1) with ∼30% of the brominated adduct. Refluxing the compound in toluene with $I_2$ (cat.) afforded the desired *E* isomer. $^1$H NMR ($CDCl_3$) 7.50−7.57 (m, 3H), 7.39 (d, $^3J$ = 8.09 Hz, 2H), 7.19 (m, 1H), 7.12 (m, 1H), 6.85 (m, 2H), 4.62 and 4.54 (s + s, 1H), 3.87 (s, 3H), 3.85 (s, 3H). $^{13}$C NMR ($CDCl_3$) 153.9, 151.7, 138.2, 137.0, 136.7, 129.7, 129.4, 129.2, 128.8, 128.7, 127.2, 127.1, 126.9, 124.3, 124.2, 114.2, 112.5, 111.9, 56.4, 56.0, 46.5, 34.0. High-resolution mass spectrometry with electron ionization (HRMS-EI) 288.0909, Δ = 2.8 ppm ($C_{17}H_{17}O_2Cl$); 332.0423, Δ = 3.3 ppm ($C_{17}H_{17}O_2Br$).

**4-(2′,5′-Dimethoxystyryl)benzyl Thioacetate (6).** In a 50 mL round-bottom flask equipped with a Teflon-coated magnetic stir bar, potassium thioacetate (68 mg, 0.60 mmol) was added to 4-(2′,5′-dimethoxystyryl)benzyl bromide (175 mg, 0.53 mmol) in DMF (10 mL) under an argon atmosphere. The mixture was stirred at room temperature for 30 min and then at 90 °C for 90 min. Upon cooling, the reaction mixture was added to water, extracted with DCM, dried, and concentrated. Chromatography on silica gel eluting with DCM in hexanes (1:1) afforded 127 mg (72%) of the title compound. $^1$H NMR ($CDCl_3$) 7.45 (d, $^3J$ = 8.14 Hz, 2H), 7.44 (d, $^3J_{trans}$ = 16.58 Hz, 1H), 7.28 (d, 2H), 7.15 (d, $^4J$ = 2.92 Hz, 1H), 7.06 (d, 1H), 6.86 (d, $^3J$ = 8.60 Hz, 1H), 6.80 (dd), 4.13 (s, 2H), 3.85 (s, 3H). 3.83 (s, 3H), 2.37 (s, 3H). $^{13}$C NMR ($CDCl_3$) 195.4, 153.9, 151.6, 137.1, 137.0, 129.3, 129.0, 127.3, 127.0, 123.6, 113.9, 112.5, 111.6, 56.5, 56.0, 33.5, 30.6. HRMS-EI: 328.1121, Δ = 3.7 ppm.

**4-(2′,5′-Dihydroxystyryl)benzyl Thioacetate (2).** In a 25 mL round-bottom flask equipped with a Teflon-coated magnetic stir bar, a 0.7 M solution of boron tribromide in DCM (1.4 mL, 1.0 mmol) was added dropwise to 4-(2′,5′-dimethoxystyryl)benzyl thioacetate (90 mg, 0.27 mmol) in DCM (5 mL) at −78 °C under an argon atmosphere with constant stirring. The mixture was allowed to warm to room temperature. After 30 min the solution was cooled to 0 °C, cold water was added, and the reaction was allowed to warm to room temperature. After 30 min, the reaction mixture was diluted with ethyl acetate (50 mL) and brine (50 mL). The organic phase was separated, then dried, and concentrated. Chromatography on silica gel eluting with ethyl acetate in hexanes (3:6) afforded 31 mg (39%) of the title compound. $^1$H NMR (acetone-$d_6$): 8.1 (br s, 1H), 7.8 (br s, 1H), 7.46−7.51 (m, 3H), 7.31 (d, $^3J$ = 8.29 Hz, 2H), 7.13 (d, $^3J_{trans}$ = 16.58 Hz, 1H), 7.08 (d, $^4J$ = 2.92 Hz, 1H), 6.75 (d, $^3J$ = 8.60 Hz, 1H), 6.63 (dd, 1H), 4.13 (s, 2H), 2.34 (s, 3H). $^{13}$C NMR (acetone-$d_6$): 195.4, 151.8, 149.4, 138.4, 130.5, 130.3, 128.8, 127.8, 127.6, 126.0, 117.8, 117.0, 113.4, 33.8. HRMS-EI: 323.0729, Δ = 3.4 ppm $(M + Na)^+$.

**4-(4′-Bromomethylstyryl)benzaldehyde (7).**[35] In a 125 mL round-bottom flask equipped with a Teflon-coated magnetic stir bar

(27) Trammell, S. A.; Spano, A.; Price, R.; Lebedev, N. *Biosens. Bioelectron.* **2006**, *21*, 1023−1028.
(28) Lowy, D. A.; Tender, L. M.; Zeikus, J. G.; Park, D. H.; Lovley, D. R. *Biosens. Bioelectron.* **2006**, *21*, 2058−2063.
(29) Flaig, W.; Beutelspacher, H.; Riemer, H.; Kalke, E. *Justus Liebigs Ann. Chem.* **1968**, *719*, 96.
(30) Bailey, S. I.; Ritchie, I. M.; Hewgill, F. R. *J. Chem. Soc., Perkin Trans. 2* **1983**, 645−652.
(31) Bishop, C. A.; Tong, L. K. J. *J. Am. Chem. Soc.* **1965**, *87*, 501.
(32) Sato, Y.; Fujita, M.; Mizutani, F.; Uosaki, K. *J. Electroanal. Chem.* **1996**, *409*, 145−154.
(33) Kwon, Y.; Mrksich, M. *J. Am. Chem. Soc.* **2002**, *124*, 806−812.
(34) Rosowsky, A.; Papoulis, A. T.; Forsch, R. A.; Queener, S. F. *J. Med. Chem.* **1999**, *42*, 1007−1017.
(35) Norinder, U.; Tanner, D.; Wennerstrom, O. *Tetrahedron Lett.* **1983**, *24*, 5411−5414.

and water-jacketed condenser, 4-bromomethylbenzaldehyde (517 mg, 2.6 mmol) and diethyl 4-(4,4,5,5-tetramethyl-1,3-dioxolan-2-yl)benzylphosphonate (1.00 g, 2.8 mmol) were added to anhydrous THF (40 mL) under an argon atmosphere with constant stirring. Potassium *t*-butoxide was added at 0 °C, and the reaction was allowed to warm to room temperature and stirred overnight. The next day, the mixture was diluted with diethyl ether (200 mL), washed with several portions of water, dried, and concentrated. The product was dissolved in a solution of THF (20 mL) in aqueous HCl (10%, 40 mL) and stirred at 65 °C for 3 h. Upon cooling, the organic phase was extracted with several portions of DCM, dried, and concentrated. Chromatography on silica gel eluting with DCM afforded 540 mg (69%) of the title compound. $^1$H NMR ($CDCl_3$) 10.00 (s, 1H), 7.88 (d, 2H), 7.65 (d, 2H), 7.52 (d, 2H), 7.41 (d, 2H), 7.24 (d, 1H), 7.15 (d, 1H), 4.61 (s, 2H).

**4-[4′-(2″,5″-Dimethoxystyryl)styryl]benzyl Chloride (8).** 4-(4′-Bromomethylstyryl) benzaldehyde (295 mg, 0.66 mmol), dimethoxybenzyltriphenylphosphonium chloride (200 mg, 0.66 mmol), and sodium hydride (18 mg, 0.75 mmol) were reacted, worked up, and separated in the same manner as previously described. Chromatography afforded 192 mg (67%) of the title compound as *E* and *Z* isomers, which were used in the next step without isomerization. $^1$H NMR *E* isomer only ($CDCl_3$) 7.48−7.57 (m, 7H), 7.40 (d, $^3J$ = 8.00 Hz, 2H), 7.19 (d, $^4J$ = 2.76 Hz, 1H), 7.13 (s, 2H), 7.12 (d, $^3J_{trans}$ = 16.43 Hz, 1H), 6.87 (d, $^3J$ = 8.91 Hz, 1H), 6.82 (dd, 1H), 4.62 (s, 2H), 3.88 (s, 3H), 3.85 (s, 3H). HRMS-EI: 390.1399, Δ = 3.1 ppm.

**4-[4′-(2″, 5″-Dimethoxystyryl)styryl]benzyl thioacetate (9).** 4-[4′-(2″,5″-Dimethoxystyryl)styryl]benzyl bromide (150 mg, 0.34 mmol) and potassium thioacetate (46 mg, 0.40 mmol) were reacted, worked up, and separated in the same manner as previously described. Chromatography afforded 117 mg (79%) of the title compound. Refluxing the compound in toluene with $I_2$ (cat.) afforded the desired *E* isomer. $^1$H NMR ($CDCl_3$): 7.45−7.55 (m, 7H), 7.29 (d, $^3J$ = 8.10 Hz, 2H), 7.17 (d, $^4J$ = 2.79 Hz, 1H), 7.10 (d, $^3J_{trans}$ = 16.51 Hz, 1H), 7.10 (s, 2H), 6.85 (d, $^3J$ = 8.93 Hz, 1H), 6.81 (dd, 1H), 4.14 (s, 2H), 3.87 (s, 3H), 3.84 (s, 3H), 2.37 (s, 3H). HRMS-EI: 430.1615, Δ = 2.9 ppm.

**4-[4′-(2″,5″-Dihydroxystyryl)styryl]benzyl thioacetate (3).** 4-[4′-(2″,5″-Dimethoxystyryl)styryl]benzyl thioacetate (110 mg, 0.25 mmol) and boron tribromide (0.72 mmol) were reacted, worked up, and separated in the same manner as previously described. Chromatography afforded 84 mg (84%) of the title compound. $^1$H NMR (acetone-$d_6$) 8.13 (br s, 1H), 7.82 (br s, 1H), 7.51−7.61 (m, 7H), 7.32 (d, $^3J$ = 8.14 Hz, 2H), 7.25 (s, 2H), 7.17 (d, $^3J_{trans}$ = 16.43 Hz, 1H), 7.11 (d, $^4J$ = 2.92 Hz, 1H), 6.77 (d, $^3J$ = 8.60 Hz, 1H), 6.64 (dd, 1H), 4.14 (s, 2H), 2.34 (s, 3H). HRMS-EI 402.1288, Δ = 0.5 ppm.

**Monolayer Deposition on Gold Coil Electrodes.** Gold coil working electrodes consisted of 14-cm lengths of 0.5-mm diameter gold wires (99.999% pure, Aldrich). The 7-cm end segment of each wire was coiled (∼3-mm diameter inner diameter). For electrochemical measurements the coiled end of each working electrode was submersed in electrolyte (2 mL). The exposed uncoiled end was connected directly to the working electrode lead of the potentiostat. Immersed geometric areas of working electrodes were typically 1.00 ± 0.05 cm$^2$. Each gold coil electrode was individually cleaned for 30 s in piranha solution ($H_2O_2$ + $H_2SO_4$, 1:3 v/v). **Caution!** Piranha is a strong oxidizer and should be handled with extreme care. Gold disk electrodes (Bioanalytical Systems, Inc., BAS, West Lafayette, IN) were cleaned by polishing to a mirror surface with 0.05-mm alumina and sonicating in deionized water. Next, both disk and coil gold electrodes were activated in 15 mL of fresh 0.1 M $H_2SO_4$, by applying 30 potential steps of 0.2 s duration between −3.0 and 3.0 V versus Ag/AgCl, 3 M KCl. Each electrode was then rinsed with amounts of 0.1 M $H_2SO_4$, and the cleanliness of the surface was assessed by cyclic voltammetry between 0.0 and 1.5 V versus Ag/AgCl, 3 M KCl, at 200 mV/s (performed in fresh 0.1 M $H_2SO_4$).

**Electrochemistry.** All electrochemical measurements were performed under a Faraday cage, in the three-electrode geometry, with a gold working electrode, a Pt counterelectrode (Bioanalytical Systems, Inc., BAS, West Lafayette, IN), and a Ag/AgCl, 3 M KCl reference electrode. A 3 mL glass cell (CH Instruments) was used, and measurements were driven by an electrochemical workstation (Model 660a, CH Instruments, Austin, TX). All voltammograms were obtained at room temperature under ambient conditions. Each voltammogram was initiated at the negative potential limit following a 2 s quiescence period. alternating current voltammetry (ACV) data were acquired with an AC amplitude of 25 mV and an increment potential of 4 mV. pH values of solutions were adjusted by the addition of 1 M HCl or 1 M NaOH to buffers containing the appropriate p$K_a$ for the desired pH, that is, 50 mM phosphoric acid (pH 3), 50 mM acetic acid (pH 4−5), 50 mM MES (pH 6−7), 50 mM Tris (pH 8−9), and 50 mM ethanolamine (pH 10−12).[36] All buffers were adjusted to an ionic strength of 0.2 M with NaCl.[36] Voltammetric peak potentials and peak currents were analyzed by means of the software provided with the potentiostat (CH Instruments).

**Ellipsometry.** Gold substrates for ellipsometry were obtained from Evaporated Metals Film Corp (Ithaca, NY), and consisted of 1-in. long × 3-in. wide × 0.04-in. thick float glass slides coated on one side with a 100 nm thick gold film over a 5 nm thick chromium adhesion layer. Such slides were cleaved into approximately 0.2 in. × 1 in. sections and cleaned in Ar plasma (15 min, 200 mTorr, 100 W RF) just prior to monolayer deposition. Clean gold substrates were modified with SAMs by immersion in 1 mM solution of each thiol derivative in ethanol, for 2 h at room temperature, and then rinsed with copious amounts of ethanol and DI water. Gold substrates were dried in $N_2$ stream prior to each measurement. Monolayer thickness was measured with a J. A. Woollam Co., Inc. multi-wavelength ellipsometer (Lincoln, NE), at 70° angle of incidence from 400 to 800 nm.[37,38] Freshly cleaned gold substrates (unmodified) were used for determining the optical constants of gold. The ellipsometric data for the SAMs were modeled by use of optical constants obtained from clean gold substrates and adding a Cauchy layer to model the SAM. An index of refraction of 1.5 was used for monolayer **1**[39] and 1.55 for monolayers **2** and **3**.[40]

## Results

**Synthesis.** Hydroquinone-terminated OPV compounds 4-(2′,5′-dihydroxystyryl)benzyl thioacetate (**2**) and 4-[4′-(2″,5″-dihydroxystyryl)styryl]benzyl thioacetate (**3**) were synthesized according to Scheme 1, by utilizing either Wittig[41] or Horner−Wittig[42] reactions for the C−C double-bond-forming step. Accordingly, 2,5-dimethoxybenzyltriphenylphosphonium chloride (**4**) was prepared in 77% yield from commercially available starting materials.[34] This compound is a key intermediate in the synthesis of $H_2$Q-OPVs as it contains a 1,4-dimethoxyphenyl functionality, which can be reduced to the hydroquinone, and owing to its phosphonium salt moiety, can be subsequently used in Wittig-type transformations.

Preparation of **2**, the two-ring $H_2$Q-OPV, begins by treating 2,5-dimethoxybenzyltriphenylphosphonium chloride with 4-bromomethylbenzaldehyde[43] under Wittig conditions to give 4-(2′,5′-dimethoxystyryl)benzyl bromide (**5**) in 71% yield. Compound **5** is produced as a mixture of *E* and *Z* isomers that can be converted to the preferred *E* isomer by thermal isomerization. It should be

(36) Beynon, R. J.; Easterby, J. S. *Buffer Solutions: The basics*; Scientific Publishers: Oxford, U.K., 1996.
(37) Stoycheva, S.; Himmelhaus, M.; Fick, J.; Kornviakov, A.; Grunze, M.; Ulman, A. *Langmuir* **2006**, *22*, 4170−4178.
(38) Colavita, P. E.; Miney, P. G.; Taylor, L.; Priore, R.; Pearson, D. L.; Ratliff, J.; Ma, S.; Ozturk, O.; Chen, D. A.; Myrick, M. L. *Langmuir* **2005**, *21*, 12268−12277.
(39) Ulman, A. *An introduction to ultrathin organic films: from Langmuir−Blodgett to self-assembly*; Academic Press: New York, 1991.
(40) Seferos, D. S.; Banach, D. A.; Alcantar, N. A.; Israelachvili, J. N.; Bazan, G. C. *J. Org. Chem.* **2004**, *69*, 1110−1119.
(41) Maercker, A. *Org. React.* **1965**, *14*, 270−490.
(42) Wadsworth, W. S. *Org. React.* **1977**, *25*, 73.
(43) Lavallee, D. K.; Xu, Z.; Pina, R. *J. Org. Chem.* **1993**, *58*, 6000−6008.

**Scheme 1. Synthesis of 2 and 3**[a]

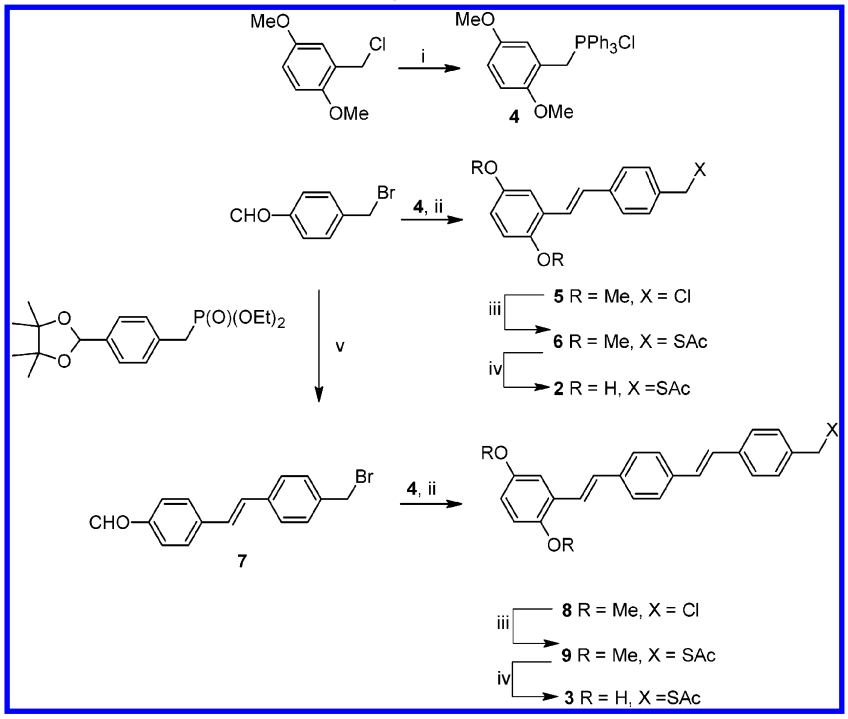


[a] Reagents and conditions: (i) triphenylphosphine, toluene, reflux; (ii) sodium hydride, THF; (iii) potassium thioacetate, DMF, 80 °C; (iv) borontribromide, dichloromethane, −78 °C; (v) (1) potassium *t*-butoxide, THF, and (2) HCl, THF, 65 °C.

noted that during the synthesis of **5**, the major product was benzyl chloride (70%) rather than the expected benzyl bromide (30%), as confirmed by MS and NMR spectroscopy. As they were not easy to separate, they were carried through to the next step. Halide displacement with potassium thioacetate proceeded smoothly to give 4-(2′,5′-dimethoxystyryl)benzyl thioacetate (**6**) in 72% yield. Finally, treatment of **6** with $BBr_3$ in dichloromethane gives 4-(2′,5′-dihydroxystyryl)benzyl thioacetate (**2**) in 39% isolated yield. Although some investigators demonstrated that these last two steps could be reversed in the synthesis of aliphatic $H_2Q$-thiols,[8,44] we were able to obtain the desired compounds only by carrying out the synthesis in this order.

The synthesis of **3**, a three-ring $H_2Q$-OPV derivative, starts by effectively extending 4-bromomethylbenzaldehyde with one phenylenevinylene unit. This extension was accomplished by treatment with 4-(4,4,5,5-tetramethyl-1,3-dioxolan-2-yl)benzylphosphonate[45] under Horner−Wittig conditions, and produced solely the desired *E*-isomer of 4-(4′-bromomethylstyryl)benzaldehyde in 69% yield. The next three manipulations, Wittig coupling with **4**, halide displacement with potassium thioacetate, and $BBr_3$ reduction, were carried out in a manner analogous to **2**, to produce compound **3** in a yield of 44% (for the three consecutive steps).

**Monolayer Characterization.** Gold electrodes and substrates were modified with SAMs of **1**, **2**, or **3** as described in the Experimental Section. Ellipsometric measurements were made to determine the average thickness of the film, which characterized the resulting SAMs, and confirmed how the molecules aligned in the monolayers. Average thickness values of the films were 1.4 ± 0.2 nm for **1**, 0.4 ± 0.2 nm for **2**, and 1.3 ± 0.2 nm for **3**. Lengths of each molecule, as estimated from optimized 3D structures (ADC/ChemSketch), were 1.78 nm for **1**, 1.16 nm for **2**, and 1.77 nm for **3**. By considering a 30° tilt angle[39] typically

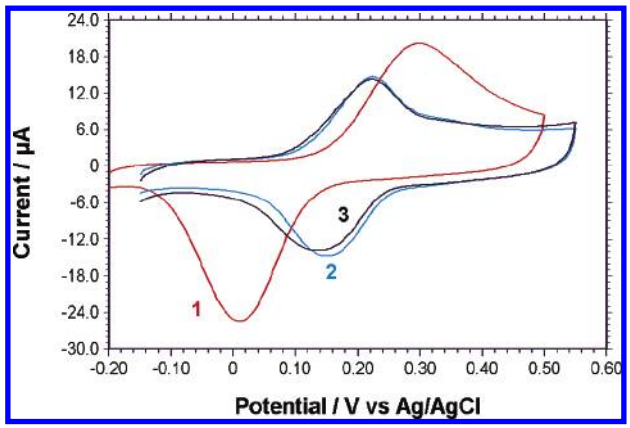


**Figure 1.** Cyclic voltammograms of SAMs on gold coil containing **1** (red), **2** (blue), and **3** (black) in a pH 4 buffer adjusted to an ionic strength of 200 mM with NaCl. Scan rate = 50 mV $s^{-1}$.

observed in alkanethiol SAMs and the a 37° tilt[46] found in conjugated thiol SAMs, we can conclude that ellipsometric thicknesses measured for SAMs of **1** and **3** were within the experimental error of the calculated value, while the thickness of **2** was lower than expected.

Cyclic voltammetry was the major technique for characterizing the monolayers; examples of typical CVs for each SAM at pH 4 and a scan rate of 50 mV/s are displayed in Figure 1. The scans reveal a single redox couple with a large peak-to-peak separation for **1** and, as expected, smaller peak-to-peak separations for **2** and **3**. The full width at half-maximum for all three CVs is ∼135 mV, which is much larger than the ideal Nernstian value for a surface-confined two-electron redox couple (45 mV); this may indicate lateral interactions between the headgroups in the monolayer.[1] However, the large peak width did not affect the accuracy of determining the peak positions, which were of primary

(44) Hickmen, J. J.; Ofer, D.; Laibinis, P. E.; Whitesides, G. M.; Wrighton, M. S. *Science* **1991**, *252*, 688−691.
(45) Bartholomew, G. P.; Rumi, M.; Pond, S. J. K.; Perry, J. W.; Tretiak, S.; Bazan, G. C. *J. Am. Chem. Soc.* **2004**, *126*, 11525−11542.
(46) Seferos, D. S.; Trammell, S. A.; Bazan, G. C.; Kushmerick, J. G. *Proc. Natl. Acad. Sci. U.S.A.* **2005**, *102*, 8821−8825.

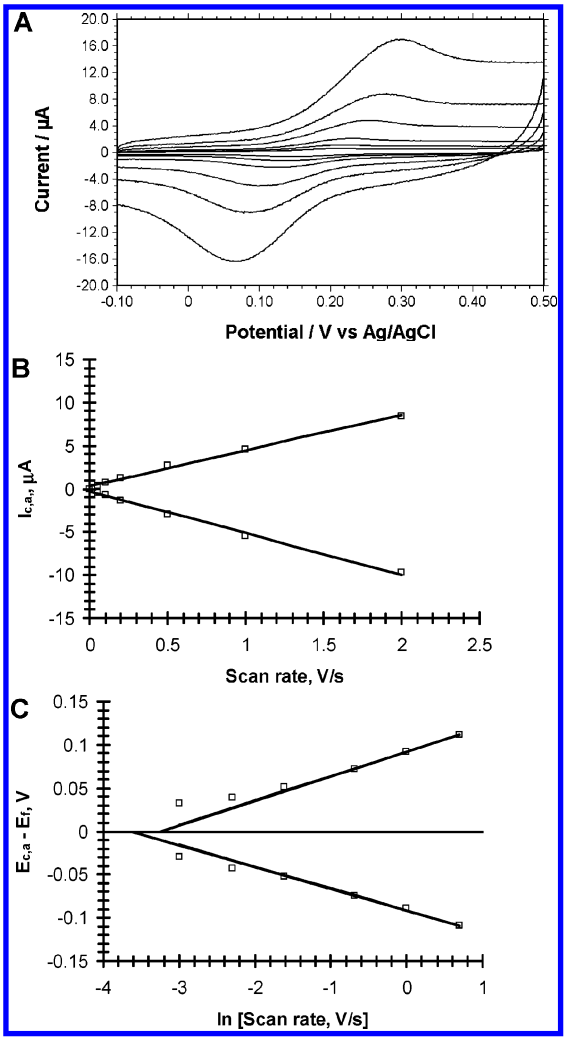


**Figure 2.** (A) Cyclic voltammograms of **2** on a gold disk as a function of scan rate. (B) Peak currents ($I_{pc}$ and $I_{pa}$) vs rate scan. (C) Peak-to-peak separation ($E_{c,a} - E_f$) vs ln (scan rate).

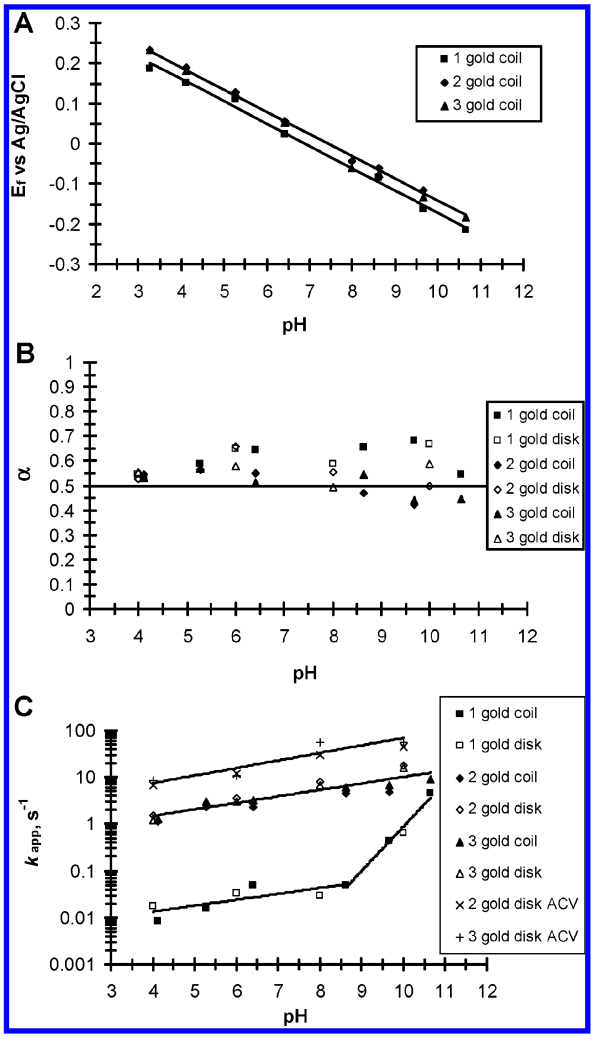


**Figure 3.** (A) Formal potential of **1**, **2**, and **3** on gold coil as a function of pH. (B) α vs pH for each SAM measured on both gold disk and coil. (C) $k_{app}$ vs pH for each SAM measured on both gold disk and coil including the ACV results.

interest to us. For all tested SAMs both the anodic ($I_{pa}$) and cathodic peak ($I_{pc}$) currents scale linearly with scan rate, which is typical of surface-bound species. An example for **2** is shown in Figure 2A with CVs recorded at scan rates of 0.05, 0.1, 0.2, 1, and 2 V/s; the linear graph of $I_{pa}$ and $I_{pc}$ versus scan rate is shown in Figure 2B.

The estimated surface coverage (Γ) for each SAM was calculated by integrating the cathodic and anodic peaks and considering the two-electron process for the $H_2Q$ couple. The geometric area of the electrode was used for the surface coverage calculation, and the surface roughness was assumed to be constant from the reproducible pretreatment of the gold coils. With these considerations, the surface coverage was approximately $4 \times 10^{-10}$ mol cm$^{-2}$ for **1** and $\sim 2 \times 10^{-10}$ mol cm$^{-2}$ for both **2** and **3**. For reference, the literature values for full monolayer coverage of hydroquinone thiols and hydroquinone alkanethiols are between 5.4 and $5.6 \times 10^{-10}$ mol cm$^{-2}$.[8] While the coverage of **1** is consistent with these values, SAMs of **2** and **3** correspond to submonolayer coverages, suggesting that the OPV bridge does not pack tightly under the conditions tested.

**Electrochemical Kinetics.** To investigate the thermodynamics and kinetics of the $Q/H_2Q$ couple contained in each SAM, we recorded CVs as a function of pH and scan rate. First, we describe the observations of the scan-rate dependence. The apparent rate constant ($k_{app}$), was determined from the peak-to-peak separation (>200 mV/$n$, where $n$ is the number of electrons exchanged) of the $Q/H_2Q$ couple by use of Laviron's formalism.[47] Critical scan rates, $\nu_a$ and $\nu_c$, were obtained by plotting ($E_{c,a} - E_f$) versus ln (scan rate) and extrapolating to ($E_{c,a} - E_f$) = 0, where $E_f$ of the $Q/H_2Q$ couple was calculated as the average of the cathodic ($E_c$) and anodic ($E_a$) peak potentials (see Figure 2C). The electron-transfer coefficient, α, was calculated from the slopes of the linear portion of each curve and averaged where the slope = $RT/\alpha nF$ for the cathodic branch and $RT/(1-\alpha)nF$ for the anodic branch. Rate constants ($k$) from each critical scan rate were calculated from eq 1 with $n = 2$. The value of $k_{app}$ was calculated as the average value of anodic and cathodic apparent rate constants for overall redox reaction:

$$k = \frac{\alpha nF\upsilon_c}{RT} = \frac{(1-\alpha)nF\upsilon_a}{RT} \qquad (1)$$

We focus next on the pH dependence of ET. For each SAM, the formal potential values, $E_f$, shift toward the negative direction with increasing pH (Figure 3A). Between pH 3 and 11, and at scan rates from 0.05 to 5 V/s, each SAM gave a Nernstian response for $E_f$ of 58 mV/pH unit, consistent with a two-electron, two-proton couple.[30] The ET coefficients (α) for **2** and **3** were approximately 0.5 with a noticeably higher value between pH

(47) Laviron, E. *J. Electroanal. Chem.* **1979**, *101*, 19−28.

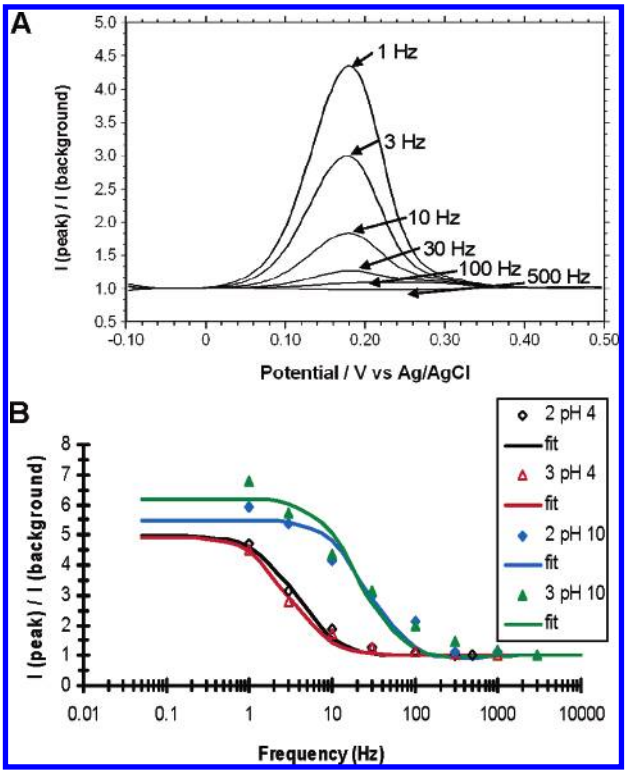


**Figure 4.** (A) ACV for **2** on a gold disk electrode at pH 4 at different frequencies. (B) $I$(peak)/$I$(background) vs frequency for **2** and **3** at pH 4 and 10 on a gold disk electrode with the simulated fitted curves.

5 and 10 for **1** (Figure 3B). CVs were recorded by use of both small (0.02 $cm^2$) and large (1 $cm^2$) area gold electrodes. From both data sets, $k_{app}$ overlaid well (Figure 3C), suggesting no significant error due to an $iR$ drop, which would distort the CVs and give erroneous peak-to-peak separations. For each SAM, log ($k_{app}$) scales linearly with pH between pH 4 and 9 (Figure 3C).[48] For **1** above pH 9, there is a clear break in the trend with a significant increase in slope of log ($k_{app}$) versus pH. When $k_{app}$ values from SAMs containing either **1** or **3** are compared, the OPV bridge shows a significant increase in $k_{app}$ (~100 fold) in the range of pH 4−9. In addition, within the same pH range, $k_{app}$ for SAMs containing either **2** or **3** appears to be independent of the length of the OPV bridge.

Due to the inherent limitations of CV determining fast ET rates, alternating current voltammetry (ACV) was used as an additional electrochemical technique to evaluate the rate constants of ET for **2** and **3**. A convenient protocol involving current−ratio data analysis as a function of the log of frequency has been used successfully for the evaluation of ET rate constants for surface-confined redox couples.[18,49,50] Following the protocol reported by Creager and Wooster,[49] ACVs were recorded over a range of frequencies (Figure 4A) and the ratio of peak to background current ($I_p/I_b$) was plotted as a function of the log of frequency (Figure 4B). Simulated curves based on a Randles equivalent circuit were used to fit the data. Fitting parameters pertaining to the resistance to charge transfer, $R_{ct}$, and adsorption pseudocapacitance, $C_{ads}$, were used to calculate values for the rate constants (see Supporting Information).[49] From the ACV analysis, $k_{app}$ was a factor of ~4 larger compared to $k_{app}$ from the Laviron analysis (Figure 3C). However, it is clear that $k_{app}$ for **2** and **3** is the same within experimental uncertainty, again pointing out that between pH 4 and 10, ET is independent of the length of the OPV bridge.

## Discussion

Between pH 3 and 11, all three SAMs containing the Q/$H_2$Q redox couple displayed a Nernstian pH dependence, with the measured formal potentials shifting by 58 mV/pH unit, consistent with a two-electron, two-proton transfer (eq 2).[31] Taking into account the deprotonation of $H_2Q$ to $HQ^-$ (eq 3) (p$K_{a1}$ = 9.85), above pH 9.85 a two-electron, one-proton couple (eq 4) would undergo a change in slope to 30 mV/pH unit.[31] Since there appears to be no change in slope above pH 9.85, we believe that the p$K_{a1}$ for $H_2Q$ (eq 3) shifts to a higher value upon surface binding.[8]

$$Q + 2e^- + 2H^+ \overset{k_{app}}{\rightleftharpoons} H_2Q \qquad \text{pH } 3-9 \qquad (2)$$

$$H_2Q \rightleftharpoons HQ^- + H^+ \qquad \text{p}K_a = 9.85 \qquad (3)$$

$$Q + 2e^- + H_2O \overset{k_{app}}{\rightleftharpoons} HQ^- + OH^- \qquad \text{pH } 9.85-11.4 \qquad (4)$$

The ET mechanism of a surface-confined two-electron, two-proton couple has been theoretically treated by Laviron,[48] by using a nine-member square scheme and assuming that ET coefficients are equal to 0.5, while the protonation is at equilibrium. Laviron's theory predicts slow apparent rate constants, which result from acid−base equilibria that favor the reactant with less favorable driving forces for ET.[48,51] Finklea[51] extended Laviron's work by maintaining the first assumption but allowing the ET coefficients to vary with potential.[51] Since surface-confined p$K_a$s and the formal potentials of the elementary ET steps are not yet known, a detailed analysis with a nine-member square scheme was beyond the scope of this work.

The ~100-fold increase in $k_{app}$ observed for OPV bridge **3** relative to alkane bridge **1** of similar length (Figure 3C) suggests that for **1** at pH 4−9, the rate-limiting step in $k_{app}$ for the two-electron, two-proton couple has a significant electron tunneling component.[8] The clear change in slope for **1** after pH 9 reveals a change in mechanism. This assumption is in agreement with a recent paper in which rate constants were found to be distance-independent at strongly basic pH for a series of $H_2Q$ molecules tethered to the electrode surface with alkanethiols of different lengths.[9] For **2** and **3**, $k_{app}$ values at pH 4−10 (Figure 3C) are very similar, implying that the rate-limiting step associated with the two-electron, two-proton couple (eq 2) is independent of the length of the OPV bridge. This suggests the rate-limiting step in eq 2 is probably related to the multiple pathways of a two-electron, two-proton transfer mechanism of the hydroquinone headgroup. However, since there is no clear break at pH 9 for **2** and **3**, the overall mechanism relating the interplay between the electron tunneling and the proton-coupled steps may in fact be more complicated.

It is interesting to note that in working at a slightly basic pH (pH = 9) to a mildly acidic pH (pH = 4), one observes a significant enhancement (~100 fold) of the ET kinetics of the OPV surface-confined $H_2Q$ redox species. This pH range represents a window that is most relevant to biological processes, and very similar conditions are likely to be employed for fabricating and operating bioelectronic devices. This observation suggests that the OPV molecules reported and studied here may provide a more efficient

(48) Laviron, E. *J. Electroanal. Chem.* **1983**, *146*, 15−36.
(49) Creager, S. E.; Wooster, T. T. *Anal. Chem.* **1998**, *70*, 4257−4263.
(50) Jhaveri, S. D.; Lowy, D. A.; Foos, E. E.; Snow, A. W.; Ancona, M. G.; Tender, L. M. *Chem. Commun.* **2002**, 1544−1545.
(51) Finklea, H. O. *J. Phys. Chem. B* **2001**, *105*, 8685−8693.

way to electronically couple biomolecules with the electrode surfaces, under conditions that are likely to be compatible with biological processes. This finding should provide motivation for using $H_2$Q-OPV molecules for the construction of efficient bioelectronic devices such as sensors and photovoltaics.

**Acknowledgment.** The research was supported by the Naval Research Laboratory. Financial support from the Institute for Collaborative Biotechnologies (D.S.S. and G.C.B.) is gratefully acknowledged. We thank Professor Stephen Creager of Clemson University for proving an Excel spreadsheet to analyze the variable-frequency AC voltammetry.

**Supporting Information Available:** Fitting parameters from the ACV analysis. This material is available free of charge via the Internet at http://pubs.acs.org.

LA061555W